Design and manufacture of 8.4 m primary mirror segments and supports for the GMT

H. M. Martin[a], J. R. P. Angel[a], J. H. Burge[a,b], B. Cuerden[a], W. B. Davison[a], M. Johns[c], J. S. Kingsley[a], L. B. Kot[a], R. D. Lutz[a], S. M. Miller[a], S. A. Shectman[c], P. A. Strittmatter[a] and C. Zhao[b]

[a]Steward Observatory, University of Arizona, Tucson, AZ 85721, USA
[b]College of Optical Sciences, University of Arizona, Tucson, AZ 85721, USA
[c]Carnegie Observatories, 813 Santa Barbara St, Pasadena, CA 91101 USA

ABSTRACT

The design, manufacture and support of the primary mirror segments for the GMT build on the successful primary mirror systems of the MMT, Magellan and Large Binocular telescopes. The mirror segment and its support system are based on a proven design, and the experience gained in the existing telescopes has led to significant refinements that will provide even better performance in the GMT. The first 8.4 m segment has been cast at the Steward Observatory Mirror Lab, and optical processing is underway. Measurement of the off-axis surface is the greatest challenge in the manufacture of the segments. A set of tests that meets the requirements has been defined and the concepts have been developed in some detail. The most critical parts of the tests have been demonstrated in the measurement of a 1.7 m off-axis prototype. The principal optical test is a full-aperture, high-resolution null test in which a hybrid reflective-diffractive null corrector compensates for the 14 mm aspheric departure of the off-axis segment. The mirror support uses the same synthetic floatation principle as the MMT, Magellan, and LBT mirrors. Refinements for GMT include 3-axis actuators to accommodate the varying orientations of segments in the telescope.

Keywords: telescopes, optical fabrication, optical testing, aspheres, mirror support, active optics

1. INTRODUCTION

The primary mirror for the Giant Magellan Telescope (GMT) consists of seven 8.4 m segments as shown in Figure 1.[1,2] A central symmetric segment is surrounded by six off-axis segments. Each segment is a honeycomb sandwich mirror similar to the 8.4 m primary mirrors of the LBT. They are the largest segments that can be made, and they guarantee a smooth wavefront over 8.4 m apertures. The GMT's secondary mirror is segmented to match the primary. Fine alignment and phasing of the separate apertures will be performed by the secondary segments.

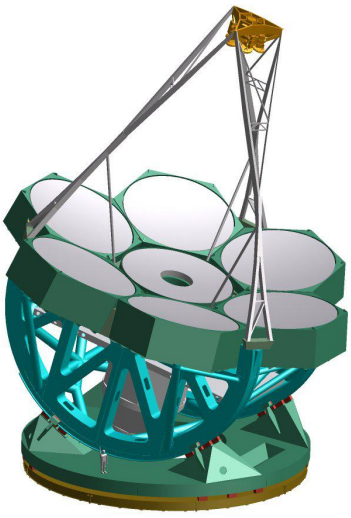

Figure 1. Model of the GMT. The seven primary mirror segments form a single parent surface, as do the matching secondary mirror segments.

Optomechanical Technologies for Astronomy, edited by Eli Atad-Ettedgui, Joseph Antebi, Dietrich Lemke,
Proc. of SPIE Vol. 6273, 62730E, (2006) · 0277-786X/06/$15 · doi: 10.1117/12.672149

The technology for the primary mirror segments and their support systems has been developed through a sequence of 3.5 m, 6.5 m, and 8.4 m mirrors produced at the Mirror Lab. Manufacture of the six outer GMT segments requires new equipment and techniques because of the off-axis aspheric surface. The project has undertaken to demonstrate the new technology early in the development phase by making the first off-axis segment. It has been cast (Figure 2) and its rear surface is currently being ground and polished. Processing of the optical surface will proceed in 2007 following construction of a new 28 m test tower that will accommodate the measurement of the off-axis segment.

Figure 2. First GMT segment resting on the furnace hearth after a successful casting.

Design of the GMT support system is proceeding in parallel with the manufacture of the segment. The system is similar to those used for the Magellan and LBT mirrors. It requires 3-axis actuators rather than 2-axis actuators because the direction of lateral forces changes with telescope elevation angle. The load spreaders that form the interface between actuators and glass have also been redesigned to avoid relying on adhesive bonds to the rear surface of the segment.

Section 2 describes the design of the segment and Section 3 discusses its requirements. Section 4 describes the fabrication process and Section 5 the measurements. Section 6 describes the manufacture of a 1/5 scale model of a GMT segment. Section 7 describes the support system and Section 8 the thermal control system.

2. DESIGN OF THE SEGMENT

The honeycomb sandwich mirror is much stiffer, yet lighter, than a comparable solid mirror. Gravitational deflections are reduced, and sensitivity to wind and actuator errors are greatly reduced. The lightweight structure and thin glass sections, combined with forced-air ventilation, reduce the mirror's thermal time constant to less than one hour, so that neither thermo-elastic deflections nor mirror seeing make a significant contribution to image blurring.

All aspects of the segment structure, shown in Figure 3, are optimized for image quality. The 28 mm facesheet thickness is about the maximum that will keep the thermal time constant under one hour. The honeycomb cell spacing of 192 mm sets the gravitational print-through of the honeycomb structure at a level of less than 10 nm peak-to-valley. The overall segment thickness is chosen to minimize deflections due to wind while keeping the segment flexible enough that manufacturing errors at low spatial frequency can be corrected with the active support system. As discussed in Section 5, the optical test of the off-axis segments has significant uncertainties in several low-order aberrations. The selected maximum thickness of 704 mm gives a mirror whose deflections due to wind are insignificant (Section 7.3) but whose shape can be adjusted to correct low-order aberrations over the range of uncertainty of the optical test. The designed mass of the segment is 16,200 kg.

The segment is made of Ohara's E6 borosilicate glass, the best material that can be cast into the complex honeycomb structure. Its expansion coefficient of 2.9 ppm/K is significant, but thermal effects are controlled by the forced-air ventilation (Section 8) and correction by the active supports. Its homogeneity in expansion coefficient, 0.005 ppm/K rms, is similar to that of ULE and Zerodur and yields insignificant deflections over the operating temperature range of +4 to +17˚C.

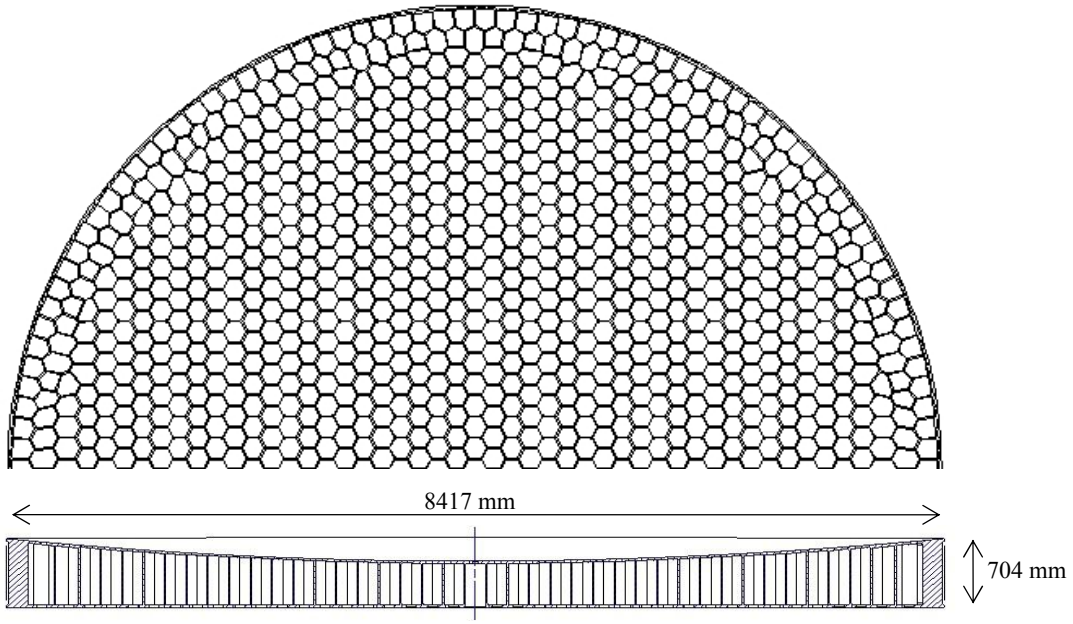

Figure 3. Half of plan view and cross section of the GMT off-axis segment.

The optical design is nearly parabolic with R = 36 m and k = -0.9983. The off-axis distance is 8.71 m to the mechanical center of the segment.

3. REQUIREMENTS FOR PRIMARY MIRROR SEGMENTS

There are two general requirements for the primary mirror segments, including their support systems and thermal control systems. The first is that wavefront errors caused by the segments should be a modest fraction of those caused by the atmosphere in the best seeing that will be encountered. For seeing-limited observations, the segment's contribution to image blurring will be small compared with the seeing limit. When adaptive optics are used, correction of wavefront errors due to the primary segments will use a small fraction of the stroke of the deformable mirror. The errors allocated to different sources are specified by their contributions to image size. For certain errors we specify or at least track the wavefront structure function, a measure of error as a function of spatial scale.

The second general requirement can be summed up as "Don't break the glass." This translates to quantitative limits on tensile stress for all load cases, including those that occur during manufacture, handling, transport, standard operation, failure of the active support system, and seismic events. Internal stresses are calculated for all of these cases, and equipment and procedures are designed to keep the maximum tensile stress below 1030 kPa (150 psi) at all times, and below 690 kPa (100 psi) for durations of more than 5 minutes. These analyses are critical to the design of the support system.

The telescope error budget is given in terms of the image diameter θ_{80} containing 80% of the energy at a wavelength of 500 nm. The terms in this error budget related to the primary mirror segments are listed in Table 1. The values apply to a zenith-pointing telescope. Errors that depend on zenith angle z are allowed to increase as the seeing increases, i. e. θ_{80} may increase in proportion to $(\sec z)^{3/5}$.

For errors that are constant over periods of minutes or longer, we assume that large-scale errors are corrected with the active optics system. Correction forces must remain within the range of the actuators, and specific limits are set on forces used to correct errors in polishing and measurement. In the analysis of different sources of error, we simulate active correction through finite-element calculations. Active correction plays a major role in the analysis of errors.[3]

Table 1. Error budget for primary mirror segments.

source of error	specification for θ_{80} (arcsec)	goal for θ_{80} (arcsec)
polishing and measuring	0.166	0.054
gravity and actuator force errors	0.036	0.036
wind	0.075	0.075
temperature gradients	0.089	0.045
mirror seeing	0.053	0.036

4. FABRICATION

4.1 Overview

Fabrication of the mirror segments follows the same strategy used for the MMT, Magellan and LBT primary mirrors.[4-6] Spin-casting creates the honeycomb sandwich structure with an accuracy of a few mm. The mirror is generated (machined) to define all critical external surfaces and bring the optical surface within about 10 μm rms accuracy. Loose-abrasive grinding and polishing of the optical surface are done with a stressed-lap polishing tool that actively conforms to the aspheric surface, augmented by small tools for local figuring.

The off-axis segments are more challenging to make than previous symmetric mirrors. The greatest challenge is accurate measurement of the off-axis surface, discussed in Section 5. Polishing is not expected to be significantly more difficult. Although the GMT segments are much more aspheric than the MMT, Magellan and LBT mirrors, the aspheric departure under the polishing tool is about the same.

Manufacture of eight GMT segments (including one spare) requires an efficient pipeline processing system that goes beyond that required for primary mirrors produced to date at the Mirror Lab. The Lab has recently expanded its facility to support this kind of processing. With the addition of a second 8.4 m polishing machine in 2004, the Lab has four stations for parallel processing of 8.4 m mirrors: the casting furnace, the generator, the polisher, and the integration area where mirror support cells are assembled and mirrors are integrated with their support systems. With each segment spending no more than 10-12 months at any station, the Lab can produce finished segments at a rate exceeding one per year after an initial ramp-up.

4.2 Requirements

The figure specification for the GMT segments is given in terms of the structure function, a representation of the error as a function of spatial scale. The specification is a seeing-limited structure function corresponding to 0.11 arcsecond FWHM seeing, or $\theta_{80} = 0.166$ arcsecond. Our experience is that any mirror that meets the structure-function specification at small scales will meet it by a wide margin at large scales, giving an actual image size much less than that corresponding to the specification. The second LBT primary achieved $\theta_{80} = 0.054$ arcsecond, and this is the goal for the GMT segment.

The GMT segments have tight tolerances on off-axis distance (2 mm, goal 1 mm) and clocking angle (rotation of the segment about its mechanical axis, 50 arcseconds). These tolerances are chosen to limit displacements of the segments relative to their cells, which are fixed in the telescope. There is also a tight requirement for matching radius of curvature among all seven segments, primarily to provide equal plate scales for imaging over the 20 arcminute field. The segments' radii must match well enough in the lab that they can be adjusted to give essentially a perfect match in the telescope.

All requirements apply to the combination of polishing and measuring errors, after optimizing the alignment of the segment in the telescope and correcting low-order aberrations with the active support system. Alignment adjustments are limited to the tolerances for off-axis distance and clocking angle, and correction forces are limited to 50 N rms over the 165 actuators. This allowance can be compared with the average axial force of 1070 N per actuator at zenith.

4.3 Fabrication process

Following the casting, the segment was lifted off the furnace hearth and placed in a vertical mounting ring, where the attached mold pieces were removed from the mirror (Figure 4). Inspection of the segment showed it to have good dimensional accuracy.

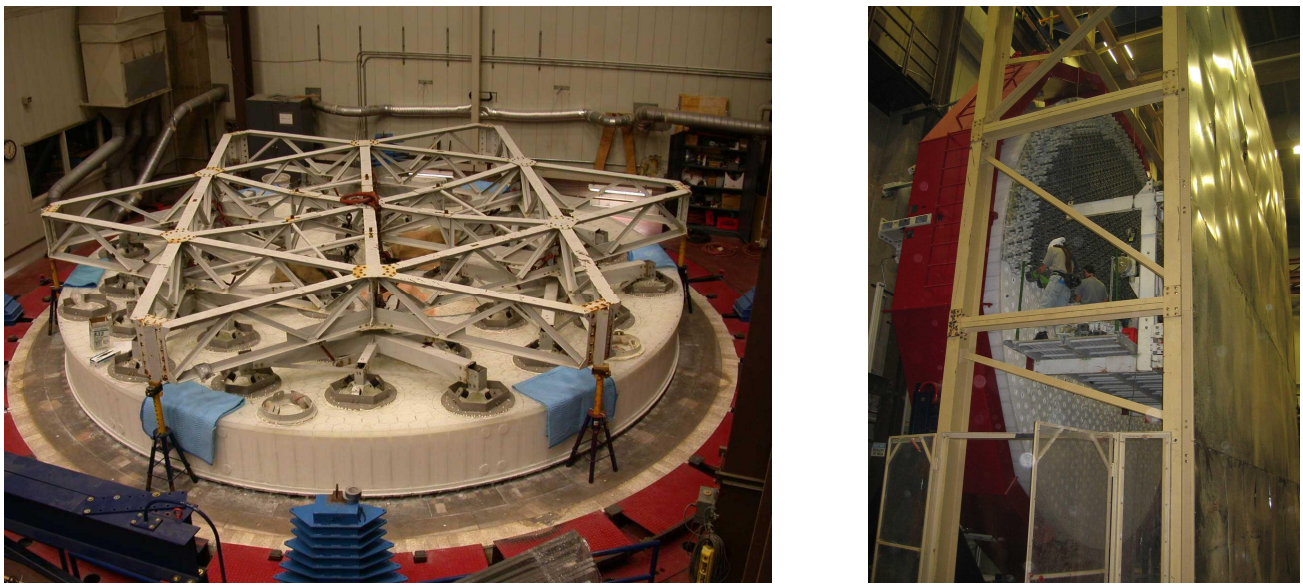

Figure 4. First GMT segment with lifting fixture attached (left) and supported vertically in the washout stand (right) where parts of the mold are removed from the segment.

The segments will be machined, or generated, to an accuracy of about 10 μm rms using a computer-controlled mill (the Large Optical Generator) that has been used to generate all large aspheric mirrors at the Mirror Lab. The off-axis shape of the front surface requires a modification of the standard generating technique, in which the tool follows a tight spiral path on the mirror as it moves from edge to center. In order to minimize the effect of backlash, we will maintain a monotonic vertical motion and weave in the horizontal direction, making the tool essentially follow contours of constant height on the aspheric surface, superposed on the spiral path.

We use a variety of lapping tools but rely heavily on a pair of 1.2 m stressed laps, shown in Figure 5. The stressed-lap system was developed at the Mirror Lab to polish and figure extremely aspheric surfaces, and it works well for off-axis as well as symmetric aspheres. The stressed lap's aluminum plate is bent elastically by computer-controlled actuators to follow the changing curvature of the aspheric surface as it moves over that surface. This allows use of a large, stiff tool with a strong smoothing action. The bending of the stressed lap required for a GMT segment, proportional to local changes in curvature of the mirror surface, is similar to that required for the Magellan and LBT mirrors, and the bending forces are somewhat less for GMT.

5. MEASUREMENT

Measurement of the off-axis surface is the greatest challenge in manufacturing the GMT segments. The test system draws on all the experience gained in the successful measurements of the highly aspheric MMT, Magellan and LBT mirrors, but the off-axis geometry calls for major innovations. A set of three tests has been defined and the concepts have been developed in some detail.[7,8] The most critical parts of the tests have been demonstrated in the measurement of a 1.7 m off-axis mirror described in Section 6.

The principal optical test is a full-aperture, high-resolution measurement of the figure, made by phase-shifting interferometry with a null corrector to compensate for the aspheric surface. The null corrector compensates for 14 mm of aspheric departure in the off-axis segment, ten times the departure of the LBT primary which is the most aspheric primary mirror in a telescope today. This results in significant uncertainty in several low-order aberrations. Ultimately, these aberrations will be measured to high accuracy in the telescope with the wavefront sensor, and the aberrations can

be adjusted both by shifting the position of the segment in the telescope and by bending it with the active supports. The fundamental requirement for the lab measurement is therefore to measure all aberrations to sufficient accuracy that the errors can be corrected in the telescope by a combination of shifting the position of the segment and bending it. The required displacement must be within the specified tolerances on off-axis distance and clocking angle, and the required correction forces must be within specified limits. The design and tolerance analysis of the GMT test show that the measurement meets these requirements.[7]

Figure 5. New 8.4 m polishing machine being used to polish the second LBT mirror. The machine has two tool carriages and can drive a variety of tools including the two 1.2 m stressed laps shown here.

Figure 6 shows the layout of the principal test. The null corrector comprises two spherical mirrors and a computer-generated hologram, that together transform the interferometer's spherical wavefront into a test wavefront matching the surface of the segment. Most of the compensation is made by an oblique reflection off a 3.75 m spherical mirror. A similar reflection off a 0.75 m sphere makes further compensation, and the hologram is designed to eliminate the residual error.

We use a scanning pentaprism test to provide an independent measurement of low-order aberrations. This test measures slope errors in a number of one-dimensional scans across the surface. A narrow collimated beam, parallel to the optical axis of the parent, is scanned across the mirror while a detector at the segment's focus monitors the position of the spot formed there. The third test uses a laser tracker to scan the surface. The laser tracker combines a distance-measuring interferometer with angular encoders and a tracking servo to follow a moving retroreflector and measure its position in three dimensions. The tracker is mounted on a fixed platform above the mirror while the retroreflector is scanned over the surface. Separate distance-measuring interferometers monitor fixed retroreflectors on the segment in order to correct for motion of the segment or laser tracker. This test will support generating and loose-abrasive grinding, and provide a meaningful independent measurement of radius of curvature and astigmatism.

For symmetric mirrors, we were able to verify the accuracy of the interferometric measurement and, in particular, the null corrector by measuring a computer-generated hologram that mimicked a perfect primary mirror. In the principal test of the GMT segment, the test wavefront is almost 4 m in diameter before it leaves the null corrector, so a verification hologram for the full null corrector is not practical. We have independent measurements of important components of the test wavefront: a small verification hologram measures and calibrates the wavefront produced by the interferometer, test hologram, and 0.75 m spherical mirror; and an interferometer measures the figure of the 3.75 m sphere from its center of curvature. We do not, however, have a direct measurement of wavefront errors due to misalignment of the 3.75 m sphere. The necessary redundancy is provided by the scanning pentaprism test, which verifies the null corrector by independently measuring low-order aberrations of the segment.

The Mirror Lab's 24 m test tower, used for center-of-curvature tests of the LBT primary mirrors as well as the MMT and Magellan 6.5 m mirrors, is not quite large enough for the principal optical test of the GMT segment. It is being replaced by a new tower shown in Figure 7 whose upper levels are wide enough to accommodate the test beam and which is stiff enough to support the 3.75 m spherical mirror and minimize vibration.

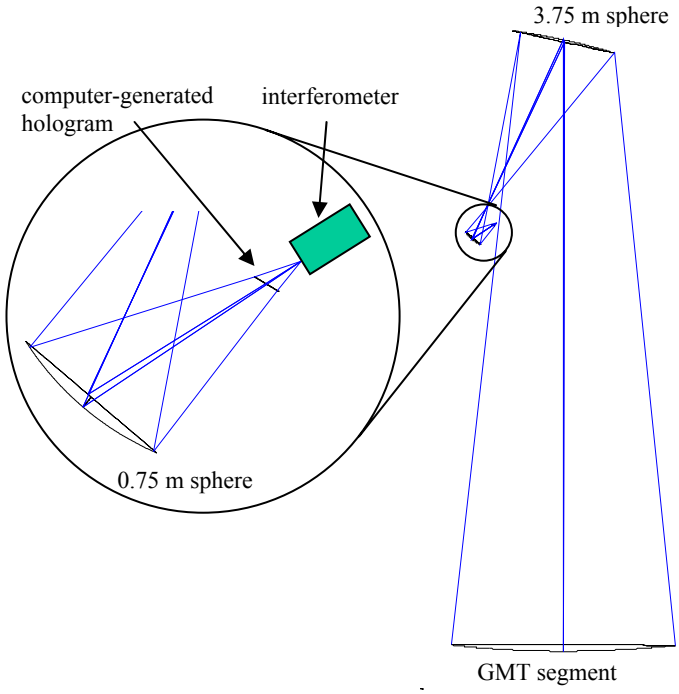

Figure 6. Layout of the principal optical test.

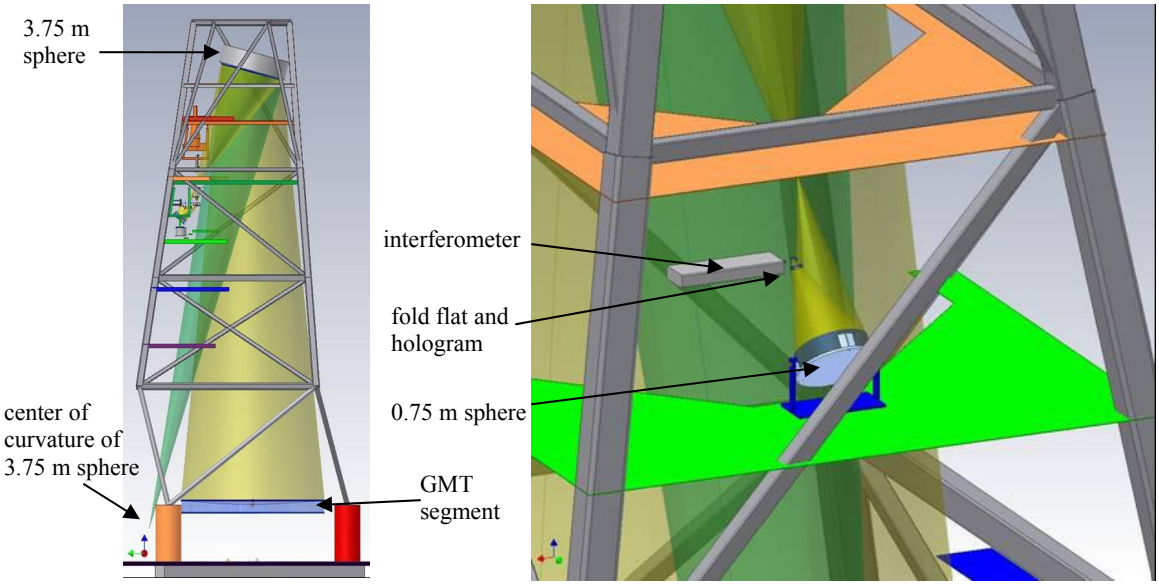

Figure 7. Design of the new test tower, showing the optics for the principal optical test of the GMT off-axis segment. Left: view showing the light cone for the GMT test and that for the simultaneous measurement of the 3.75 m fold sphere from its center of curvature. Right: close-up showing the interferometer, hologram and 0.75 mm spherical mirror for the GMT principal test.

6. MANUFACTURE OF A 1/5 SCALE PROTOTYPE MIRROR

Most of the critical technology for the off-axis GMT segments has been developed and demonstrated on a smaller scale through the manufacture of the 1.7 m off-axis primary mirror for the New Solar Telescope (NST) at Big Bear Solar Observatory. This mirror, with a radius of 7.7 m and an off-axis distance of 1.84 m, is approximately a 1/5 scale model of a GMT segment.

The manufacture of the NST primary mirror is described in detail in Ref. 9. We are figuring the NST mirror with a combination of stressed-lap polishing and local figuring with passive tools. The principal optical measurement is a full-aperture interferometric test similar to that for the GMT segment. Loose-abrasive grinding and initial polishing were guided by measurements made with a laser tracker. These measurements were accurate to about 1 μm rms surface and made it possible to resolve fringes easily in the first optical measurement of the polished surface.

The null corrector comprises a 0.5 m spherical mirror and a computer-generated hologram. Alignment of these components must be accurate to about 10 μm in three dimensions over a distance of about 1 m. We have developed techniques to achieve this alignment accuracy using metering rods and alignment references produced by the hologram.[10] We experienced some delays in implementing the alignment techniques, so figuring of the mirror was suspended between January and May 2006. The mirror's figure accuracy as of December 2005 was 32 nm rms surface after removal of some low-order aberrations that will be controlled by the active supports. Further improvement is expected after the alignment of the test optics is refined.

7. SUPPORT SYSTEM

7.1 System design

The active support system controls the segment's shape to high accuracy with relatively simple pneumatic actuators. The support system follows the same principles used for the MMT, Magellan and LBT mirrors.[11] It is a synthetic floatation system with six hard points and 165 actuators (for the off-axis segments), as shown in Figure 8. The hard points sense the net forces and moments on the segment, and the actuators apply compensating forces. The bandwidth of this outer control loop is greater than 1 Hz, so it provides excellent resistance to wind in terms of rigid body motion as well as bending.

All 165 actuators have axial components (perpendicular to the back of the segment) and 85 have lateral components (parallel to the back) as well. Four of the off-axis segments tilt around both axes, so they require two components of lateral force. The 85 actuators with lateral components therefore have 3 axes. The off-axis segments and their support cells are identical and interchangeable, so all six have the same arrangement of single-axis and 3-axis actuators.

The actuators are actively controlled to take the force of the mirror—weight, wind load, and inertia—and to bend out low-order distortion measured by the wavefront sensors in the focal plane. The forces applied by the hard points are measured and resolved into three net forces and three net moments. For each component of net force or moment there is a set of actuator forces that compensates it while minimizing deformation of the optical surface. These force patterns—including axial and both lateral components—are applied through an outer control loop operating with a bandwidth greater than 1 Hz. Additional axial force patterns are applied to correct distortions detected by the wavefront sensors at intervals of 30 seconds to several minutes. The resulting force set is checked against safety criteria to ensure that commanded forces will not result in excessive stress in the mirror.

In keeping with the design of the MMT, Magellan and LBT support systems, axial and lateral support forces are applied to the back plate of the segment. This arrangement is mechanically simpler and safer than applying forces inside the honeycomb structure near the neutral surface. The lateral forces at the back plate apply an unwanted moment to the segment, but it is easily compensated with axial forces. The axial forces therefore have a component proportional to the cosine of the segment's zenith angle (the standard axial component) and a component proportional to the sine of that angle (the compensation for lateral forces). Both components are optimized to minimize deflections of the optical surface.

Axial forces are applied under rib intersections of the honeycomb structure, where the local strength and stiffness are greatest. A spacing of 384 mm, or two honeycomb cells, between support points reduces support print-through to an insignificant level. This results in about 400 axial support points, more than the number of actuators needed to control the shape of the mirror. Most support points are therefore connected in groups of 2, 3, or 4 by load spreaders, reducing the number of actuators to165.

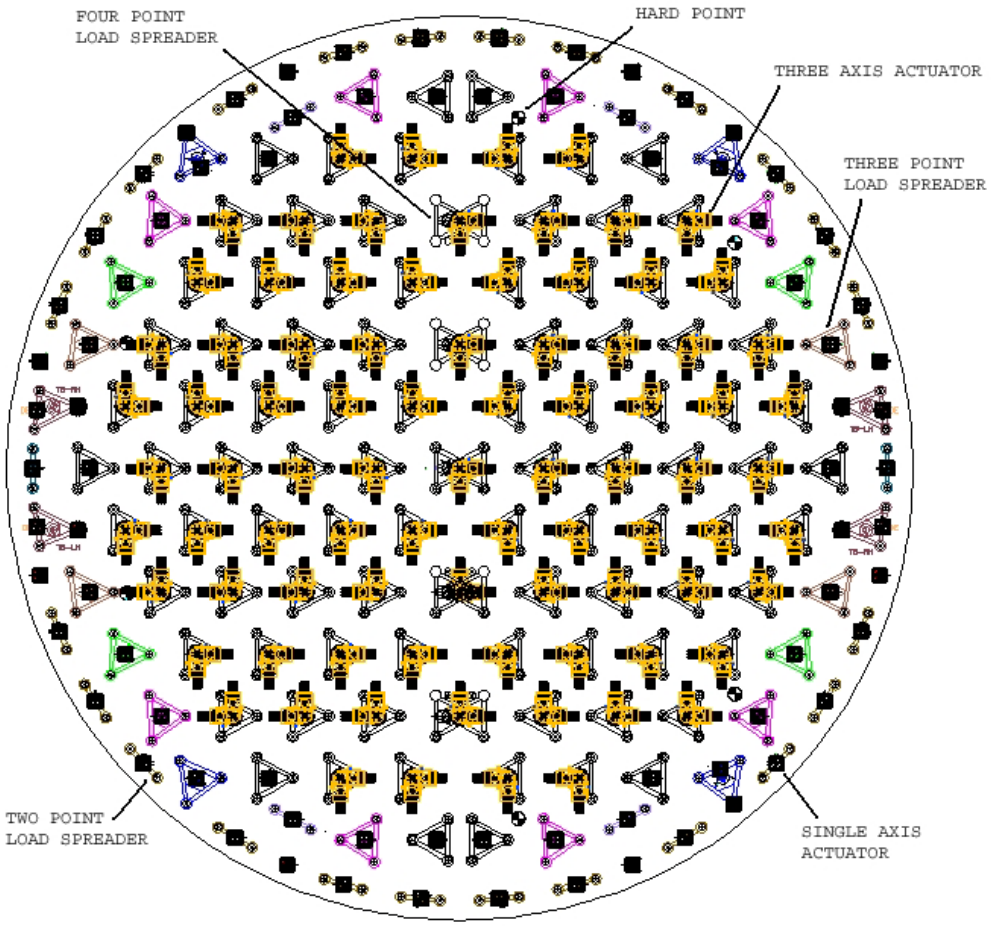

Figure 8. Layout of the segment support system.

Because the axial forces are optimized for all orientations, the distribution of lateral forces can be chosen for simplicity and to minimize local stress in the glass. Lateral forces are applied only at the locations of axial actuators that have 3- or 4-point loadspreaders. We use equal lateral forces at 85 locations covering most of the back plate. Lateral forces are applied directly in the plane of the back plate, in the holes of the back plate. Each load spreader distributes the lateral force over 3 holes.

The actuators are pneumatic force actuators. They apply axial and lateral forces in any direction. We explored several 3-axis actuator geometries, and determined that the design shown in Figure 9 is the simplest one that meets all requirements. It has one axis perpendicular to the back plate and two axes at 45˚ to the back plate. Each axis has two opposed pneumatic cylinders to provide push and pull forces. The force of each axis is measured by a load cell and controlled by a pair of proportional control valves, one for each cylinder. The load cells for all 3 axes are connected to a common plate attached to the load spreader.

7.2 Gravity and support errors

Axial forces are optimized to minimize gravity deflections for a zenith-pointing segment and a horizon-pointing segment. During manufacture, the segment will be measured zenith-pointing with a set of axial forces nominally identical to the operational forces. The gravity deflections will be polished out, causing the figure error to be zero at zenith-pointing. As the segment is tilted away from zenith, the figure error contains terms proportional to the horizon-pointing gravity deflection and the negative of the zenith-pointing gravity deflection. Figure 10 shows the figure error at a segment zenith angle of 60˚, in both directions relative to the line of symmetry of the support system. The rms surface error is 10 nm and 11 nm for the two cases.

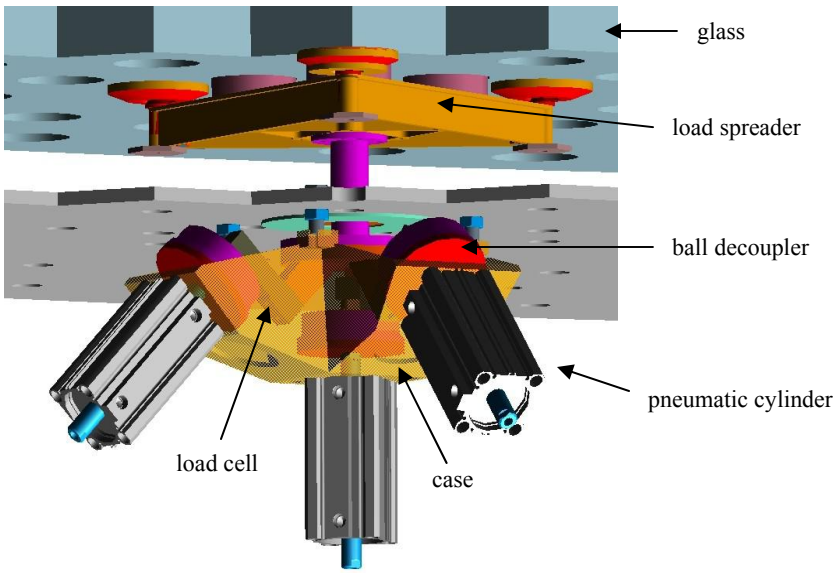

Figure 9. Conceptual design of 3-axis actuator. Each axis consists of a pair of opposed pneumatic cylinders applying force to the load spreader through a cylindrical ball decoupler and a load cell. The actuator case is attached to the upper plate of the cell, while the moving parts attach to the load spreader.

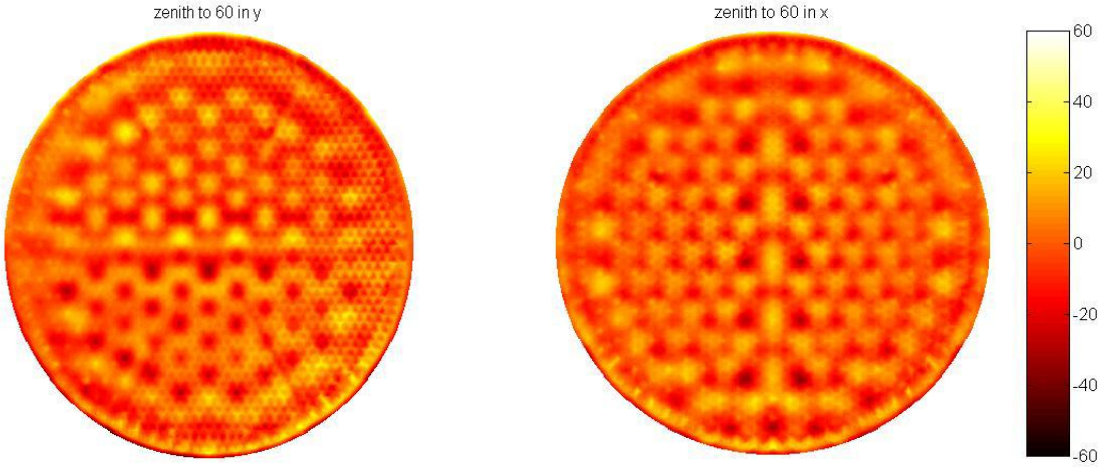

Figure 10. Figure error due to gravity deflections for a segment zenith angle of 60˚ in both directions with respect to the support layout. Apparent print-through of the honeycomb structure in the image at left is a computational artifact.

7.3 Wind deflections

An important function of the hard points is to resist the high-frequency components of wind. The low-frequency components, resisted by the full set of actuators, cause an insignificant deflection of the optical surface because the wind pressure is less than 1% of the gravity load. The locations and angles of the hard points are optimized to minimize both rigid-body displacements and deformations due to the high-frequency component. The magnitude of deflection depends on the wind speed and spectrum of fluctuations, and the bandwidth of the outer control loop that transfers reaction forces from the hard points to the actuators.

We computed deflections due to an 8.9 m/s wind with a Kaimal spectrum incident on the mirror. This gives a very conservative approximation of deflections due to wind, because the enclosure will attenuate the wind by a significant factor. The spectrum was filtered according to a 0.95 Hz outer-loop bandwidth, yielding pressure variations of

6 Pa rms for the high-frequency component. Figure 11 shows the surface deflection due to this pressure resisted by the hard points. The rms deflection is 31 nm and the smoothly varying deflection contributes insignificant image blurring.

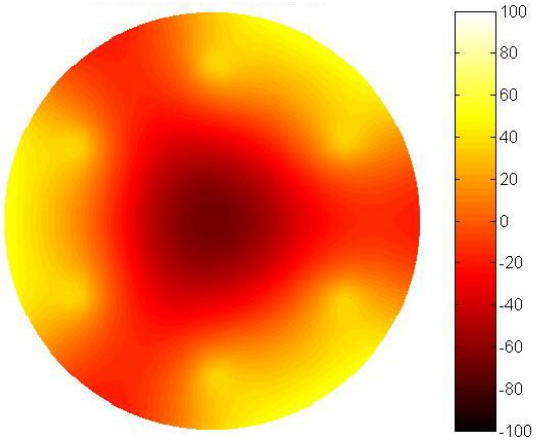

Figure 11. Deflection in nm due to the high-frequency component of an 8.9 m/s wind resisted by the hard points.

8. THERMAL CONTROL

The borosilicate mirror segment, with a thermal expansion coefficient of 2.9 ppm/K, is sensitive to temperature gradients. Gradients are minimized by ventilation of the internal structure of the segment with forced air at controlled temperature (typically ambient temperature). The ventilation system also minimizes mirror seeing by keeping the surface temperature close to ambient. The system is designed to satisfy the image error budget when the outside temperature is changing by up to ±0.5 K/h (20^{th} - 90^{th} percentile conditions).

We have calculated the deflections resulting from a number of temperature distributions. For each set of deflections we simulated a correction with the active optics system, using up to 28 bending modes for compensation. As the number of bending modes increases, the residual deflection decreases and the correction forces increase. It is necessary to strike a balance between excessive correction forces and excessive figure error. The image budget ($\theta_{80} = 0.089$ arcsecond for thermal distortion) allows rms surface errors of 35-50 nm on the spatial scales of 1-2 m that dominate the residual error after active correction. We set a limit of 50 N rms correction force over all actuators. The most problematic distribution is a uniform axial gradient. According to the analysis it must be kept below 0.12 K/m to avoid exceeding the limits on figure error and correction forces. Axial gradients that vary across the radius or diameter are more benign and can be 3-4 times larger.

The ventilation system injects air into the cells through 25 mm diameter nozzles at speeds of 12-16 m/s, giving a flow of 6-8 L/s per cell. The Magellan telescopes use fans with heat exchangers to draw air down from above the top plate of the cell and bring it to the set-point temperature close to ambient. The heat exchangers are supplied with liquid coolant from chillers off the telescope. The baseline design for GMT is a refinement of the Magellan design. Each unit supplies 18-20 nozzles at 94 Pa for the target flow rate of 8 L/s per nozzle. GMT will require about 95 ventilators per segment including the provision for 70 nozzles at the side walls.

The goal is to reduce the internal temperature gradient below 0.12 K/m. Experimental results for a case relevant to GMT (8 L/s air flow, 0.25 K/h cooling rate) showed a total variation of 0.08 K within a cell and less than 0.02 K front-to-back differences.[12] It remains to be demonstrated that this result scales to a higher cooling rate. It is likely that for the highest cooling rates the atmospheric seeing will be poor and mirror deflection will not be a limiting factor.

In the next phase of the project we will develop a full thermal model of the segment and its cell, and apply realistic heat loads as opposed to simple, defined temperature distributions. We are encouraged by the fact that the Magellan telescopes—with similar borosilicate honeycomb mirrors and a relatively weak ventilation system—regularly produce excellent images. The Magellan performance is often limited by temperature gradients in the first few hours of

the night when the mirrors are farthest from equilibrium with the ambient air. GMT needs to improve on this performance, possibly by increased ventilation flow and pre-conditioning during the daytime. The overall experience with Magellan, however, gives us confidence that the segment design is fundamentally sound and that excellent performance can be obtained without a dramatically different approach to thermal control.

9. SUMMARY

All aspects of the GMT mirror segments build on the successful primary mirror systems of the MMT, Magellan and Large Binocular telescopes. This experience gives the project a tremendous head start in the design of the mirror system, including the active support. The conceptual design is well established and attention is focused on the details. Fabrication of the first segment is well underway. Measurement of the off-axis segments is recognized as a serious challenge, and a set of measurements that meet the requirements has been defined and analyzed. Several of the critical technologies have been tested in the manufacture of a 1.7 m off-axis segment.

REFERENCES

1. M. Johns, R. Angel, S. Shectman, R. Bernstein, D. Fabricant, P. McCarthy and M. Phillips, "Status of the Giant Magellan Telescope (GMT) Project", in *Ground-based Telescopes*, ed. J. M. Oschmann, SPIE 5489, p. 441 (2004).
2. M. Johns, "The Giant Magellan Telescope (GMT)", in *Ground-based and Airborne Telescopes*, ed. L. M. Stepp, Proc. SPIE 6267 (2006).
3. H. M. Martin, B. Cuerden, L. R. Dettmann and J. M. Hill, "Active optics and force optimization for the first 8.4 m LBT mirror", in *Ground-based Telescopes*, ed. J. M. Oschmann and M. Tarenghi, SPIE 5489, p. 826 (2004).
4. B. H. Olbert, J. R. P. Angel, J. M. Hill and S. F. Hinman, "Casting 6.5-meter mirrors for the MMT conversion and Magellan", in *Advanced Technology Optical Telescopes V*, ed. L. M. Stepp, Proc. SPIE 2199, p. 144 (1994).
5. H. M. Martin, R. G. Allen, J. H. Burge, L. R. Dettmann, D. A. Ketelsen, S. M. Miller and J. M. Sasian, "Fabrication of mirrors for the Magellan Telescopes and the Large Binocular Telescope", in *Large Ground-based Telescopes*, ed. J. M. Oschmann and L. M. Stepp, Proc. SPIE 4837, p. 609 (2003).
6. H. M. Martin, R. G. Allen, B. Cuerden, J. M. Hill, D. A. Ketelsen, S. M. Miller, J. M. Sasian, M. T. Tuell and S. Warner, "Manufacture of the second 8.4 m primary mirror for the Large Binocular Telescope", in *Optomechanical Technologies for Astronomy*, ed. E. Atad-Ettedgui, J. Antebi and D. Lemke, Proc. SPIE 6273 (2006; these proceedings).
7. J. H. Burge, L. B. Kot, H. M. Martin, C. Zhao and R. Zehnder, "Design and analysis for interferometric testing of the GMT primary mirror segments", in *Optomechanical Technologies for Astronomy*, ed. E. Atad-Ettedgui, J. Antebi and D. Lemke, Proc. SPIE 6273 (2006; these proceedings).
8. J. H. Burge, T. Zobrist, L. B. Kot, H. M. Martin and C. Zhao, "Alternate surface measurements for GMT primary mirror segments", in *Optomechanical Technologies for Astronomy*, ed. E. Atad-Ettedgui, J. Antebi and D. Lemke, Proc. SPIE 6273 (2006; these proceedings).
9. H. M. Martin, J. H. Burge, S. M. Miller, B. K. Smith, R. Zehnder and C. Zhao, "Manufacture of a 1.7 m prototype of the GMT primary mirror segments" in *Optomechanical Technologies for Astronomy*, ed. E. Atad-Ettedgui, J. Antebi and D. Lemke, Proc. SPIE 6273 (2006; these proceedings).
10. R. Zehnder, J. H. Burge and C. Zhao, "Use of computer-generated holograms for alignment of complex null correctors", in *Optomechanical Technologies for Astronomy*, ed. E. Atad-Ettedgui, J. Antebi and D. Lemke, Proc. SPIE 6273 (2006; these proceedings).
11. P. M. Gray, J. M. Hill, W. B. Davison, S. P. Callahan and J. T. Williams, "Support of large borosilicate honeycomb mirrors", in *Advanced Technology Optical Telescopes V*, ed. L. M. Stepp, Proc. SPIE 2199, p. 691 (1994).
12. A. Y. S. Cheng and J. R. P. Angel, 1988. "Thermal stabilization of honeycomb mirrors", in *ESO Conference on Very Large Telescopes and Their Instrumentation*, ed. M.-H. Ulrich, ESO Conference and Workshop Proceedings N. 30, p. 467 (1988).